Phase Change in PEM Fuel Cells

Nanophase Models

Ottawa – May 12, 2006

Stephen Paddison	University of Alabama, Hunstville
Keith Promislow	Michigan State University
Greg Swain	Michigan State University
Mark Tuckerman	New York University
Guo Wei Wei	Michigan State University

Talk Overview

I) Transient Unit Cell Models
- Phase change in porous media
- Multiphase flow
- Comparisons to data
- Transient simulations

II) Hysteresis and Lateral Diffusion
- Benziger's STR Data
- Ignition waves
- Stability analysis of a toy model

III) Nanophase Models
- Proton Transport and Nanophase Separation
- Catalyst Layer Mixing
- Multiphase Performance
- Carbon Corrosion/Pt dissolution

Ionomer Membrane Properties

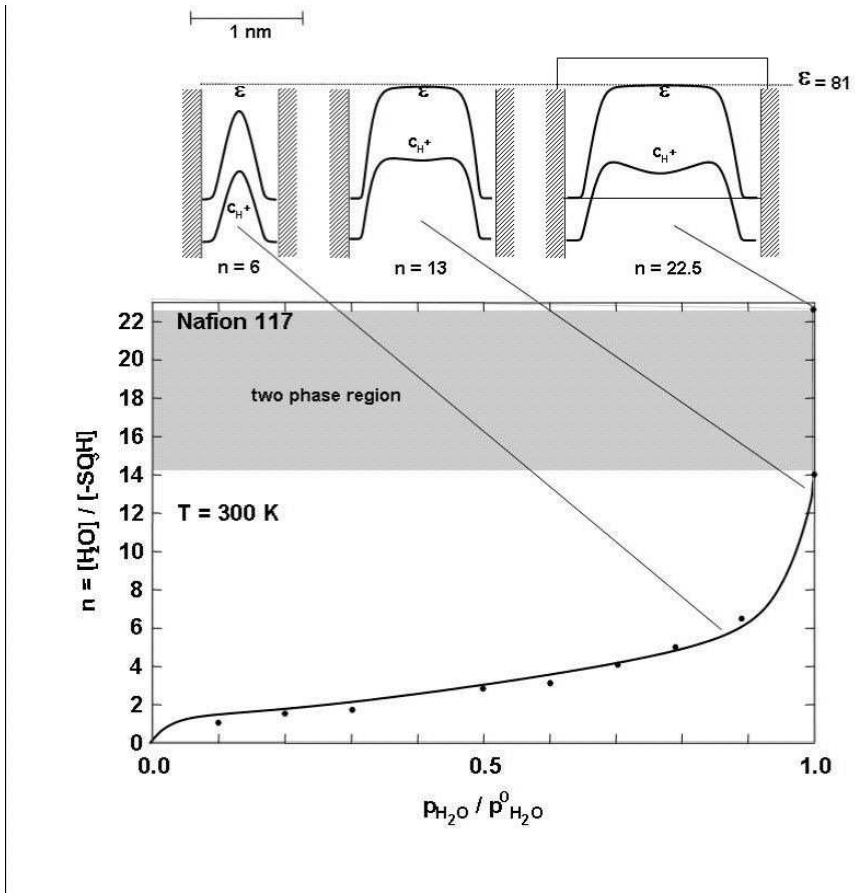

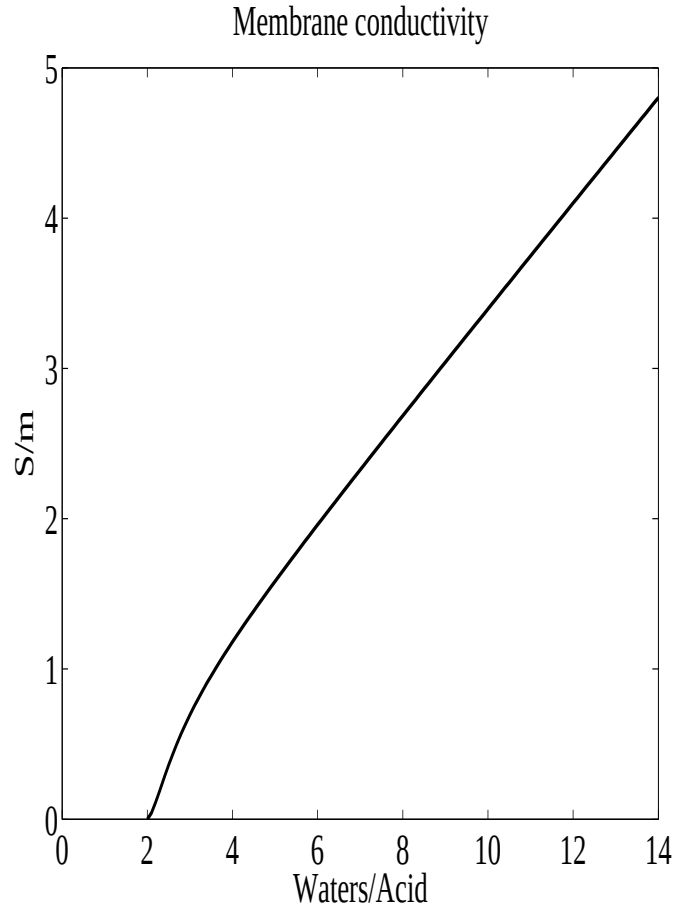

(Left) The hydration isotherm for Nafion 117.

(Right) Protonic conductivity as a function of water content.

Proton Transport in Nanophase Separated Ionomer

Why is the protonic conductivity of the membrane so sensitive to hydration?
What features of the membrane impact its conductivity?
How does external compression impact membrane water uptake?
How does one reasonably model the conduction process?
Development of high temperature membranes ($T > 120C$).

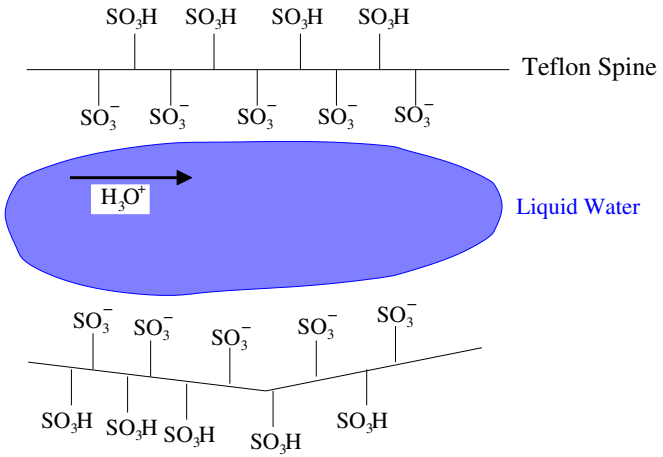

Nafion is hydrophobic, cross-linked polymer with hydrophilic (acidic) side-chains. Nafion phase-separates in presence of water forming a nano-scale liquid domain.

Based on SAX data Hsu and Gierke (1981) (1983) postulated that a balance of elastic deformation and hydrophillic surface interactions leads water to form spherical hydrophillic clusters of 4nm radius surrounded by sulfonate groups, with the clusters connected through cylindrical channels of 1nm diameter.

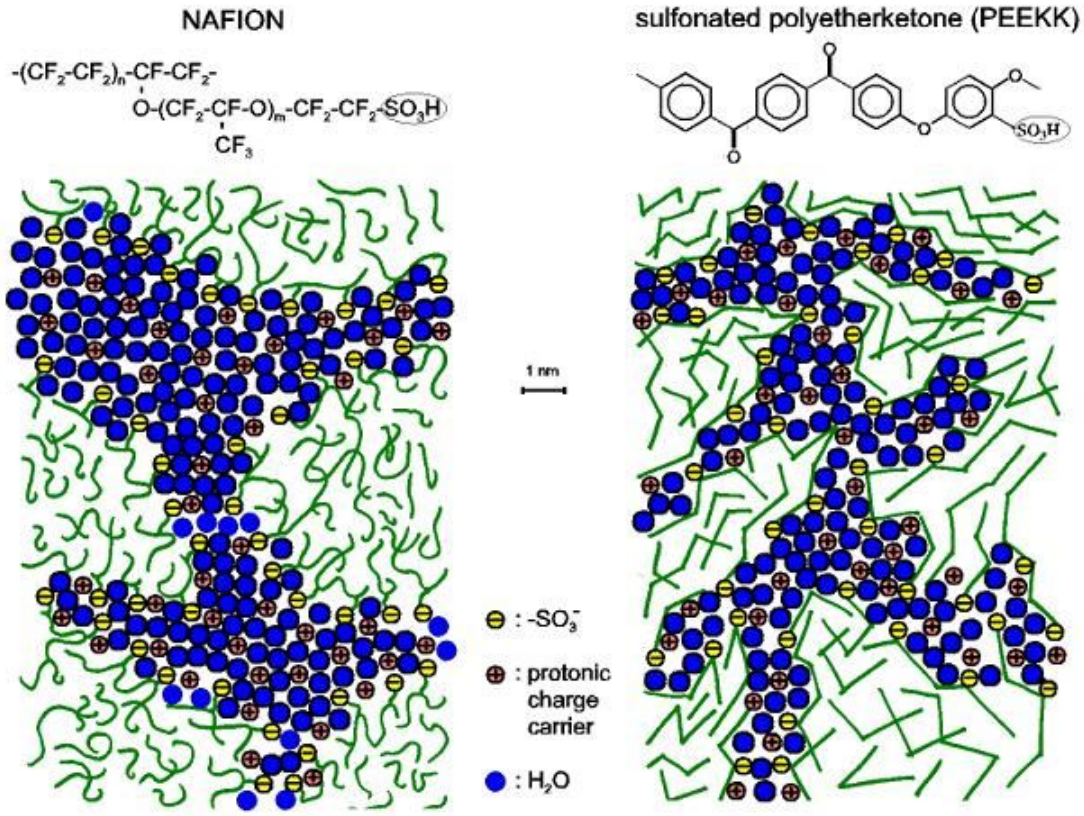

Two-dimensional illustration of the channel nano-structural features of Nafion (left inset) and PEEKK (right inset)

K.-D. Kreuer, “On the development of proton conducting polymer membranes for hydrogen and methanol fuel cells,” *J. Memb. Sci.* **185** (2001) 29.

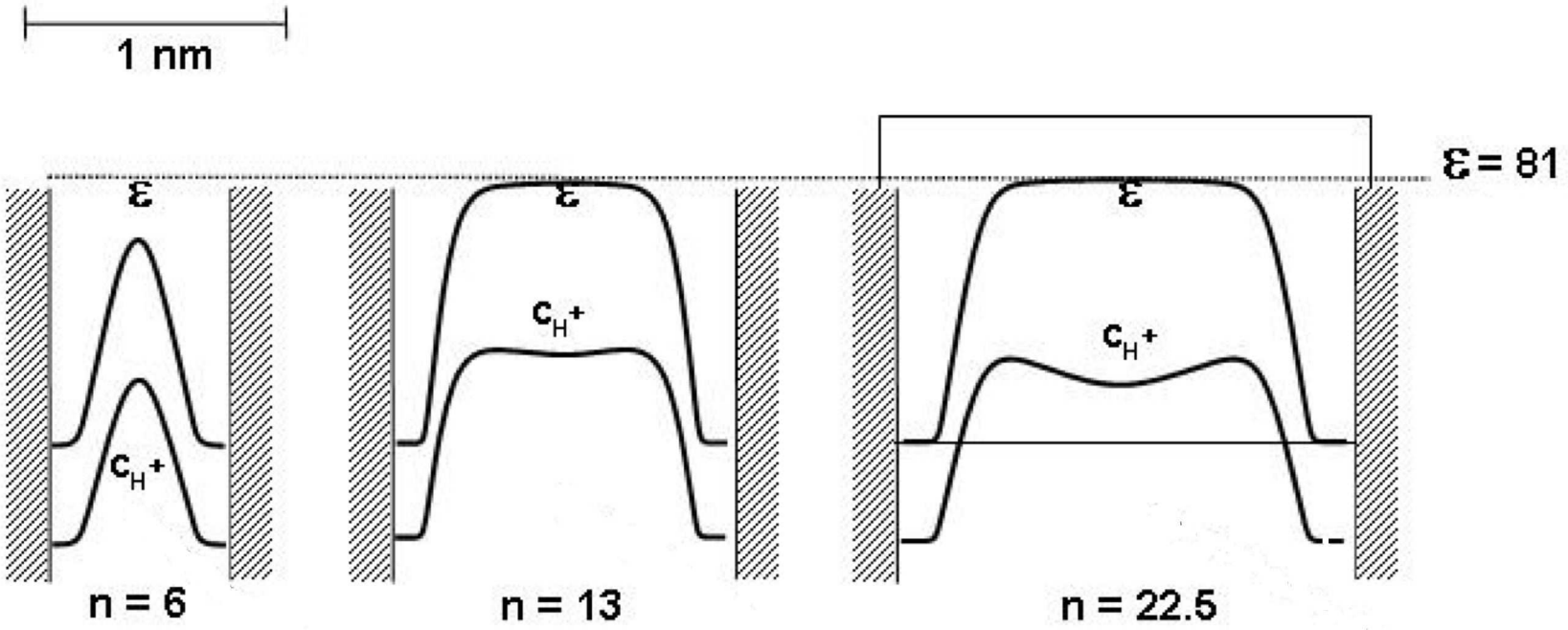

Profiles of the dielectric constant and protonic charge carrier concentration in a hydrated hydrophilic channel (pore) at three different water contents. Segregation of cationic and anionic charges leads to exceptional proton mobility.
K.-D. Kreuer, S. J. Paddison, *et. al.*, *Chem. Rev.* **104** (2004) 4637.

Nanophase Models for Ionomer Membranes

Modify ideas of C. Liu and N. Walkington, *Arch. Rat. Mech. Anal.*, **159** (2001) 229-252

Phase function: $\psi = 1$ liquid pore, $\psi = -1$ hydrophobic backbone.

Pull the Lagrangian deformation of the elastic polymer back into Eulerian coordinates and solve a "seemless" PDE for fluid and elastic polymer.

The acid groups dissociate only in the boundary layer $-1 < \psi < 1$.

Protons congregate only in the "bulk" water, $\psi = 1$.

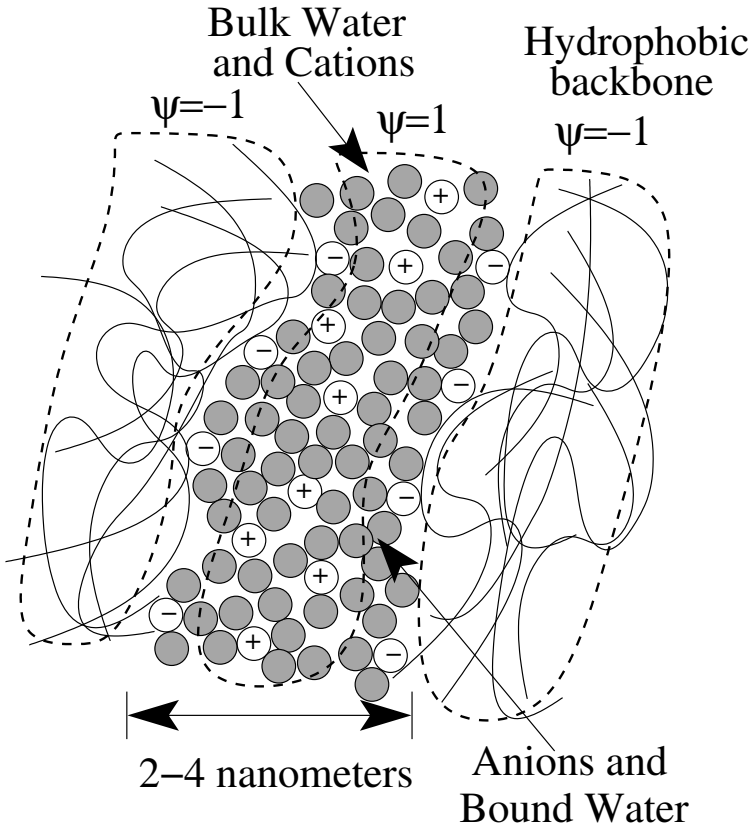

$x = x(X, t)$ Eulerian deformation in terms of Lagrangian X.

$v = x_t$ Local velocity.

$F = \frac{\partial x}{\partial X}$ Deformation gradient

Evolution equation for deformation and indicator function

$$F_t + v.\nabla F = (\nabla v)F \qquad \dot{\psi} = \psi_t + v.\nabla\psi = 0$$

Elastic Energy

Due to cross linking the membrane deforms elastically on 10-100 nanometer length scales Stress-strain energy density $\mathcal{W}(\boldsymbol{F})$. The membrane is incompressible, $\det \boldsymbol{F} = 1$, Net uptake of water results in volume expansion (swelling). The Piola-Kirchhoff stress tensor

$$(\mathcal{D}\mathcal{W})_{ij} = \frac{\partial \mathcal{W}}{\partial \boldsymbol{F}_{ij}}.$$

Small deformations of the hydrophobic domain, $\boldsymbol{F} = \boldsymbol{I} + \boldsymbol{E}$ with $\|\boldsymbol{E}\| \ll 1$.

$$\mathcal{D}\mathcal{W} = \mathcal{D}\mathcal{W}(\boldsymbol{I})(\boldsymbol{I} + \boldsymbol{E}) + \mathcal{C}(\boldsymbol{E}) + o(\|\boldsymbol{E}\|^2)$$

The Cauchy stress tensor is given by

$$\mathcal{C}(\boldsymbol{E})_{jk} = \frac{\partial^2 \mathcal{W}}{\partial \boldsymbol{F}_{il} \partial \boldsymbol{F}_{jk}} \boldsymbol{E}_{il}$$

The presence of residual stresses, $\mathcal{D}\mathcal{W}(\boldsymbol{I})$, can be induced by pretreatments of the membrane, such a boiling, but in general we assume they are zero.

Interfacial Energy Density

Smooth the Phase Function

$$\Psi_\epsilon(x) = \eta_\epsilon * \Psi \equiv \int_\Omega \Psi(y)\epsilon^{-3}\eta\left(\frac{y-x}{\epsilon}\right) dy$$

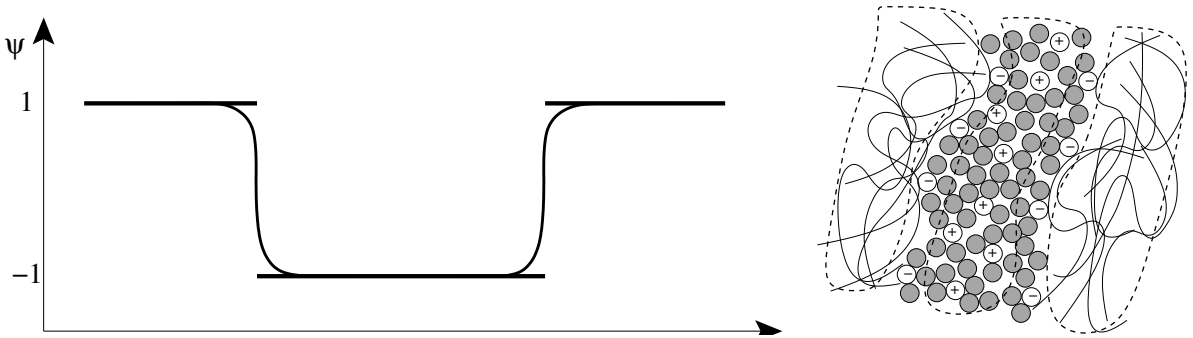

Interfacial energy dominates at 0.5-5 nanometer length-scales

$$\mathcal{I}(\psi_\epsilon) = \kappa H^2(\psi_\epsilon) - \alpha\mathcal{A}(\psi_\epsilon)$$

- κ Elastic modulus of the polymer backbone, distinct from the effective moduli which characterize $\mathcal{W}$
- α Energy density coefficient for the interface, proportional to the acid group molar density.

Square of mean curvature

$$H^2 = \int_\Omega \epsilon\left(\Delta\psi_\epsilon - \frac{1}{\epsilon^2}(\psi_\epsilon^2 - 1)\psi_\epsilon\right)^2 dx$$

Surface area

$$\mathcal{A} = \int_{\Omega} \epsilon \left(|\nabla \psi_\epsilon|^2 + \frac{1}{4\epsilon^2}(\psi_\epsilon^2 - 1)^2 \right) \, dx$$

The length scale ϵ controls the thickness of the hydrophobic-hydrophilic transition region.
The variational derivative

$$\frac{\delta \mathcal{I}}{\delta \psi_\epsilon} = \epsilon[\kappa \Delta^2 \psi_\epsilon + \alpha \Delta \psi_\epsilon] - \frac{2}{\epsilon}[\kappa(3\psi_\epsilon^2 - 1)\Delta\psi_\epsilon + \kappa\Delta\{(\psi_\epsilon^2 - 1)\psi_\epsilon\} + \alpha(\psi_\epsilon^2 - 1)\psi_\epsilon] + \frac{2\kappa}{\epsilon^3}\psi(\psi_\epsilon^2 - 1)(3\psi_\epsilon^2 - 1).$$

Competition between positive contributions from curvature balances against the negative (curvature enhancing) contributions to interface formation selects a length scale $l_0 = 1/k_0 = \sqrt{\frac{2\kappa}{\alpha}}$ for phase separation.

Force Balance

The balance between elastic, electrostatic, and interfacial forces drives the flow

$$\rho(\psi)\left(v_t + v.\nabla v\right) + \chi_l \nabla \pi \;=\; \nabla \cdot (\mu(\psi)\nabla v) + (C_- - C_+)\nabla\phi + \chi_m \nabla \cdot (\mathcal{W} F^T) + \frac{\delta \mathcal{I}}{\delta \psi}\nabla\psi$$

$\chi_l = \frac{1}{2}(1-\psi)$	liquid indicator
$\chi_m = 1 - \chi_l$	membrane indicator
$\rho = \chi_l \rho_l + \chi_m \rho_m$	density
$\mu = \chi_l \mu_l + \chi_m \mu_m$	viscosity
π	pressure conjugate to incompressibility $\nabla \cdot v = 0$
$C_-(\psi_\epsilon) = 4a(1-\psi_\epsilon)^2$	anion charge density

The electric field ϕ couples to the flow through the ion densities from Poisson's equation

$$\nabla \cdot (\varepsilon(\psi)\nabla\phi) = \frac{C_- - C_+}{\lambda^2},$$

The Debye length λ is roughly $0.5 - 1$ nanometer.
Dielectric const ε varies from 2 to 80.

Proton Transport

Where are the protons and how do they flow?

Hydrogen bound networks, Grotthuss mechanisms, vehicular transport

Approach 1 **Empirical valence-bond models** (extended Hückel type model) in which a series of N valence-bond states $|\Phi_0\rangle, \ldots, |\Phi_{N-1}\rangle$ are introduced to describe (empirically) the chemical bonding patterns that can result from the reactivity. Determine pico-second time-averaged charge densities of C_+ cations given the shape of the phase-separated domains and distribution of C_- anions.

Approach 2 **Brute force:** Insert a potential $V(\psi)$ which is supported on the $|\psi| < 1$ region. This serves to "localize" the cations within the bulk channel domains while accounting for pinching effects when channels get narrow.

$$\partial_t C_+ + \nabla \cdot \left(-D_+ \nabla C_+ - \frac{F}{\mathcal{R}T} D_+ C_+ \nabla \phi - V'(\psi) \nabla \psi_\epsilon \right) = -\partial_t C_-$$

Total charge is conserved – protons are produced by creation of interface and rapidly are pushed into the channels at high water content.

Model Properties

The Chan-Hilliard type equation

$$\Psi_t + v \cdot \nabla \Psi = \Delta \frac{\delta \mathcal{E}(\Psi)}{\delta \Psi}$$

smooths so that Ψ represents a volume fraction of phases.

The key advantage of smoothing the phase function is that we maintain separation of phases while permitting interactions between phases.

Consider a Toy Model

$$\begin{aligned} \Psi_t + v \cdot \nabla \Psi &= 0 \\ v + \nabla \pi &= -\frac{\delta \mathcal{E}(\Psi_\epsilon)}{\delta \Psi} \nabla \Psi_\epsilon \\ \nabla \cdot v &= 0 \end{aligned}$$

Since the phase velocity is divergence free the area of the level sets of Ψ is conserved, however the amount of interface can grow or shrink. The governing equations conserve phases.

Ψ flows according to the incompressible projection of the regularized energy gradient.

As an illustrative example consider $\mathcal{E}(f) = \|\nabla f\|_{L^2}^2$, then

$$\Psi_t = \diamond \left[(\Delta \eta_\epsilon * \Psi)(\nabla \eta_\epsilon * \Psi) \right] \cdot \nabla \Psi$$

where $\diamond$ is the divergence free projection.

"Mesa's of phase interacting through tails like cheerios floating in milk"

Open Questions

In what contexts does the energy

$$\mathcal{I}(\Psi) = \kappa H^2(\Psi_\epsilon) - \alpha \mathcal{A}(\Psi_\epsilon)$$

possess minimizers?

If there is no driving force, then $v = 0$ and one may view the steady form of the force balance as an Euler-Lagrange equation for the total energy

$$\mathcal{E}(\psi, F) = \mathcal{W}(F) + \mathcal{I}(\psi) + \mathcal{V}(\psi, \phi),$$

where both F and ψ are known in terms of the deformation map $x(X)$ from an "unstressed" reference configuration to the minimizer, and

$$\mathcal{V} = \int_\Omega |\varepsilon(\psi_\epsilon)\nabla\phi|^2 dx$$

is the contribution of the induced electric field to the energy.

Can the electric field coupling be expressed in a closed form at a reasonable level of approximation?

Does this energy have minimizers, what are the appropriate constraints? What structure does the minimizing set possess?

Catalyst Layer Mixture Models

Figure 1

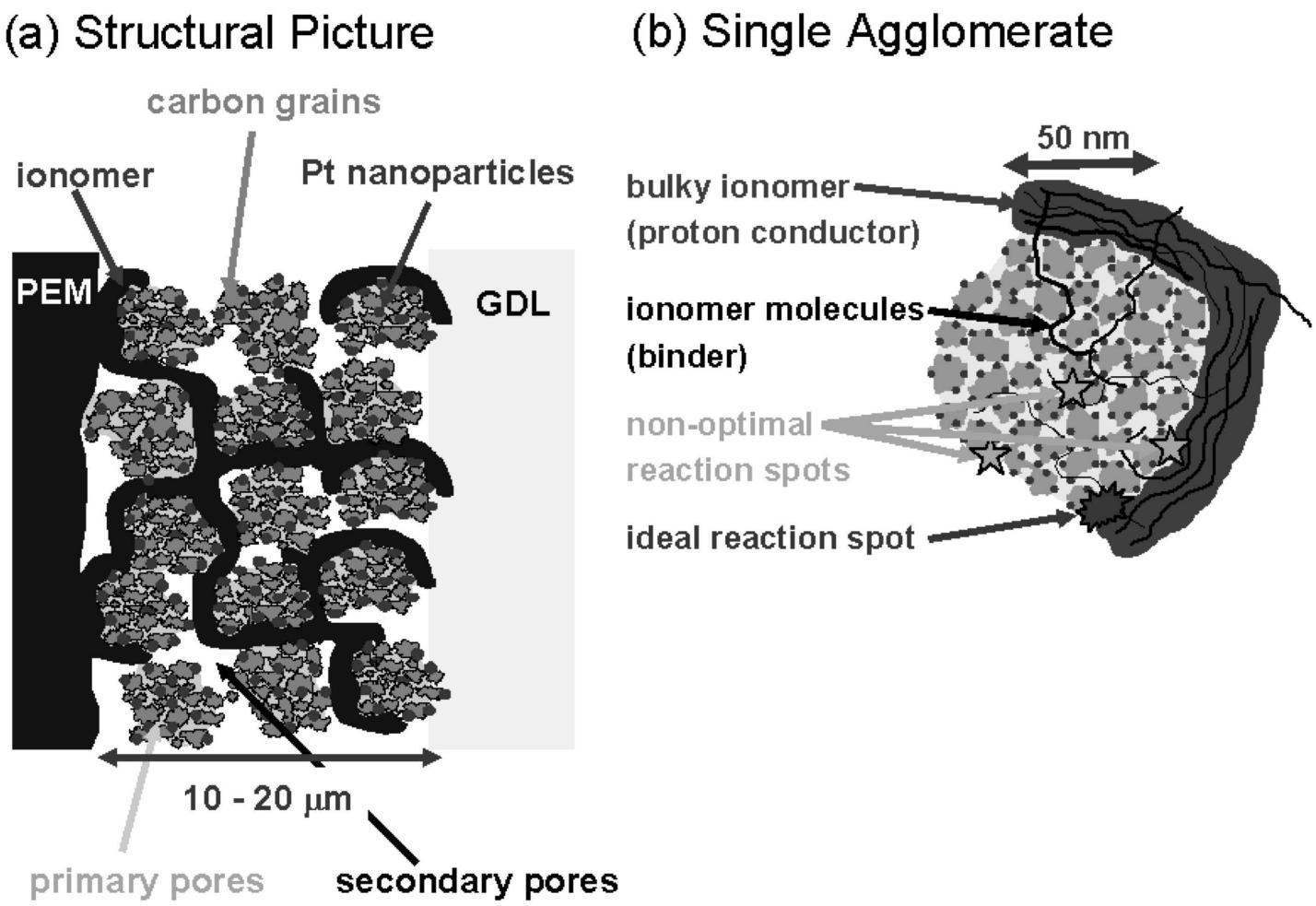

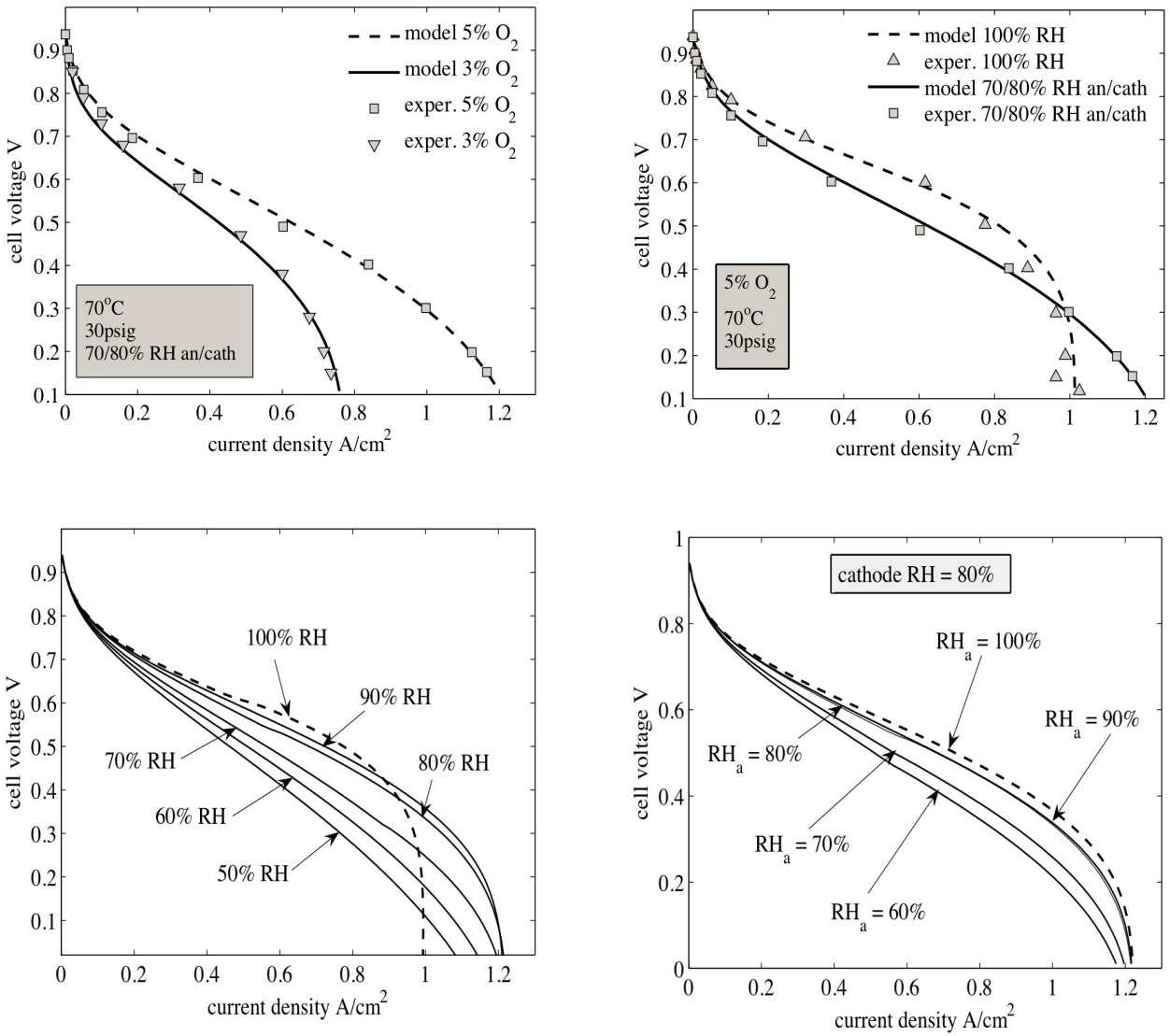

Polarization curves at (top left) Two different O_2 conc. (top right) two channel RHs (bo ttom left) 6 channel RHs with equal anode and cathode RH (bottom right) 5 anode RHs with cathode RH=80%. Joint work with Akeel Shah/John Stockie/G. S. Kim. Macro-scale models can fit data but cannot guide development.

Catalyst Layer Models

AN APPROXIMATE MODEL FOR MASS TRANSFER WITH REACTION IN POROUS GAS DIFFUSION ELECTRODES

M. B. CUTLIP*
Department of Chemical Engineering, University of Connecticut, Storrs, Connecticut 06268, U.S.A.

(*Revised version received* 16 *December* 1974)

Abstract—An approximate model for reactant mass transfer in fuel cell electrodes has been formulated which considers gaseous diffusion in the hydrophobic Teflon phase, diffusion across a thin electrolyte film at the surface of the catalyst phase, and internal diffusion with first order reaction in the electrolyte-filled catalyst phase. An analytical solution is presented which indicates the fraction of the "activation only" current density that is obtained from the electrode. Application of this model for low reactant concentrations should allow a more quantitative evaluation of important mass transfer processes in fuel cell electrodes.

Preparation Models: Resolve 5-50 nanometer scale of the ionomer/electrolyte and carbon support mixing process which fixes the catalyst nanoscale structure. Validate against SAX experiments (Andre Lee)

Performance Models: Determine the impact of the catalyst layer structure on heat and mass transport, including generation of liquid water regions and ionomer swelling

Degradation Models: Include additional reactions for carbon corrosion, Pt dissolution with accompanying phase change.

In a 500 nanometer cube, track phase domains for carbon, ionomer, gas, liquid. Include interfacial energies (surface tension), van der Waals interactions, elastic energy, electrostatic interactions, to provide a force balance model for the mixing, phase change, transport and reaction which resolves down to the 5 nanometer length-scale.

Preparation Models

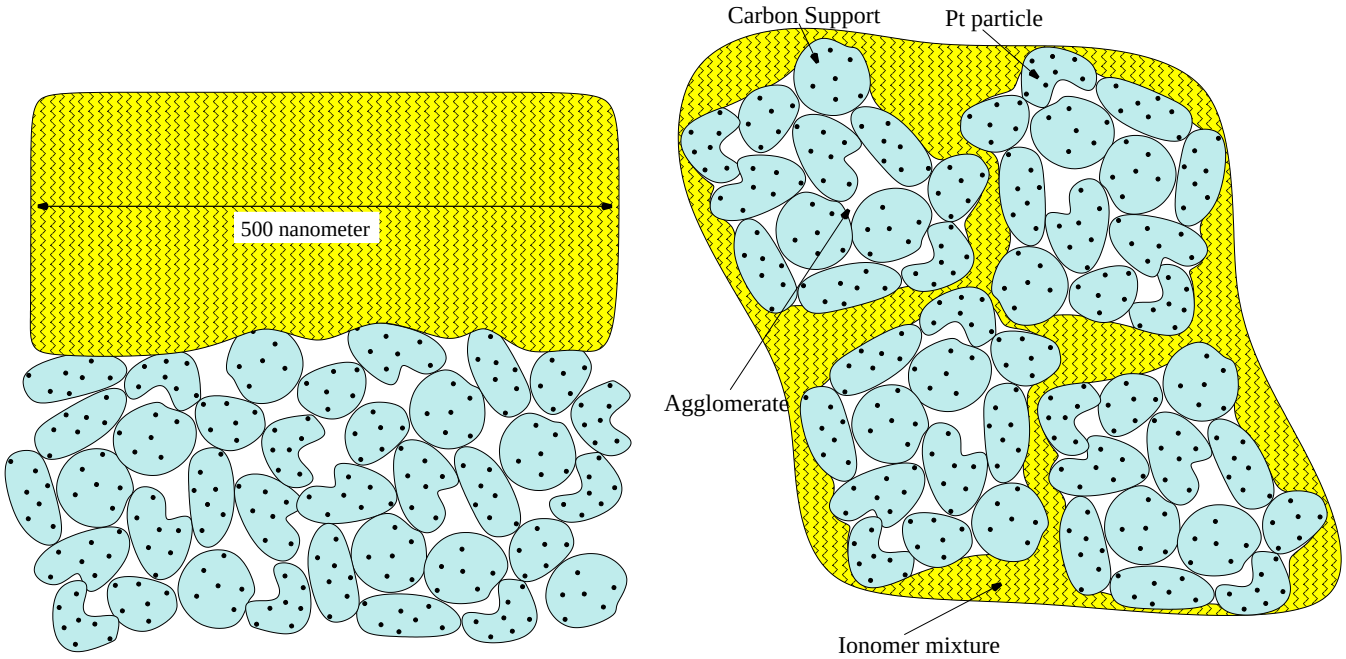

Carbon support is comprised of 30-40 nanometer carbon black particles with 5-10 nanometer Pt catalyst inclusions decorating the surface.

Carbon particulates naturally congregate into 150-250 nanometer agglomerates due to residual charges and surface interactions.

Agglomerated carbon is mixed with an aqueous polymer alcohol solution forming the catalyst ink.

How does surface wettability of carbon support/viscosity of polymer impact polymer interpenetration?

How should the external forces be optimized to mix “well”?

Preparation Model Details

Key Ideas:

Don't track interfaces Don't Impose BCs	Introduce a phase function ψ which takes three distinct values $\{\psi_s, \psi_i, \psi_g\} \subset \mathbf{R^2}$. to indicate whether $\psi(x)$ is solid, ionomer, or gas.
All Eulerian	Elastic deformation is naturally Lagrangian, but it can be pulled back into an Eulerian framework – write an *evolution* equation for the elastic deformation tensor.

Interfacial Energy

ϵ – interfacial length scale

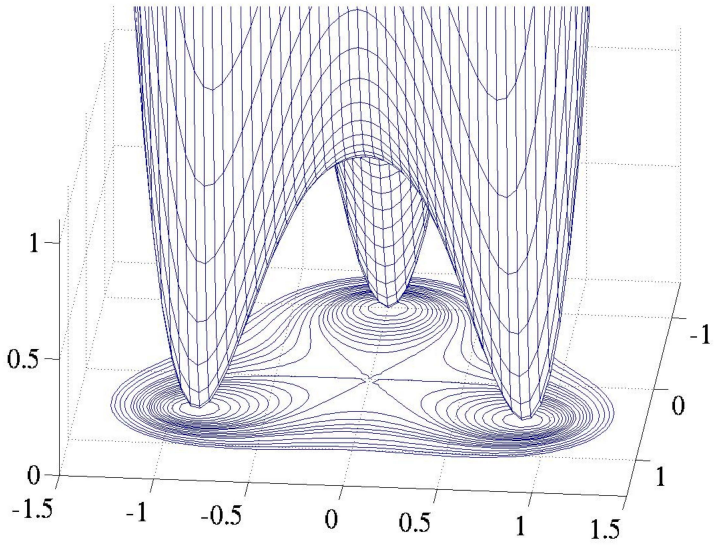

$$\psi_t + v.\nabla\psi = 0,$$

$$\nabla \cdot v = 0$$

$$\psi_\epsilon = \int_\Omega \frac{1}{\epsilon^3}\eta\left(\frac{y-x}{\epsilon}\right)\psi(y)dy,$$

$$\mathcal{I}_\epsilon = \int_\Omega \epsilon\left(|\nabla\psi_\epsilon|^2 + \frac{1}{\epsilon^2}W(\psi_\epsilon)\right)dx,$$

Elastic Energy

The motion of the material is described by the deformation map $\boldsymbol{x} = \boldsymbol{x}(\boldsymbol{X}, \boldsymbol{t})$, giving the location $\boldsymbol{x}$ of Lagrangian particle $\boldsymbol{X}$ at time $\boldsymbol{t}$.

Material velocity	$\boldsymbol{v} = \dot{\boldsymbol{x}},$
Strain of solid phase	$\boldsymbol{F}_{ij} = \frac{\partial \boldsymbol{x}_i}{\partial \boldsymbol{X}_j},$
Incompressibility	$\det \boldsymbol{F} = 1,$
Strain-Energy function	$\mathcal{W} = \mathcal{W}(\boldsymbol{F}),$
Piola-Kirchhoff stress tensor	$(\mathcal{D}\mathcal{W})_{ij} = \frac{\partial \mathcal{W}}{\partial \boldsymbol{F}_{ij}},$

Evolution for $\boldsymbol{F}$, compatibility between deformation and velocity,

$$\boldsymbol{F}_t + (\boldsymbol{v}.\boldsymbol{\nabla}\boldsymbol{F}) = (\boldsymbol{\nabla}\boldsymbol{v})\boldsymbol{F}.$$

Inter-particle attractivity

Agglomeration driven by residual charges/weak surface bonding modeled by a van der Waals potential

$$\mathcal{N}(\boldsymbol{x}) = \sum_{k \neq k_0}^{N_c} \left(\frac{\boldsymbol{\alpha}}{(\boldsymbol{x}_k - \boldsymbol{x})^M} - \frac{\boldsymbol{\beta}}{(\boldsymbol{x} - \boldsymbol{x}_k)^N} \right)$$

where $\boldsymbol{x}_k$ is center of k'th carbon support and point $\boldsymbol{x}$ is inside particle $\boldsymbol{k}_0$.

Force Balance for velocity

The mixture flows in response to body forces, elastic, interfacial, and electrostatic energy

$$\rho(v_t + v.\nabla v) + \nabla\pi - \nabla\cdot(\mu(\psi)Dv) + \frac{\delta\mathcal{I}_\epsilon}{\delta\psi_\epsilon}\nabla\psi_\epsilon + \chi_s\left(\nabla\cdot(\mathcal{D}\mathcal{W}(F)F^T) + \nabla\mathcal{N}\right) = \rho f$$

Body force driving mixing	f
Indicator function for phase p	χ_p
Pressure	π, conjugate to incompressibility
Density	$\rho = \rho_s\chi_s(x) + \rho_i\chi_i(x) + \rho_g\chi_g(x)$
Viscosity	$\mu = \mu_s\chi_s(x) + \mu_i\chi_i(x) + \mu_g\chi_g(x)$

Performance/Degradation Models

Upscale material properties to Macroscopic transport parameters

Material properties	Carbon support size, Surface wettability, Inter-particle attractivity, Volume fractions
Macroscopic transport parameters	Electronic and Protonic conductivities, Effective Pt surface area, Oxygen transport limitations, corrosion rates

Understand the dependence of macroscopic parameters on operating conditions: liquid water formation, ionomer swelling, oxygen starvation

Include transport and reaction of scalars $\boldsymbol{U} = (\boldsymbol{U}_1, \ldots, \boldsymbol{U}_{n_s})$ including oxygen, dissolved oxygen, protons, heat, liquid water, vapor
Reaction generates change of phase volumes, particularly liquid

Change of Phase:

The phase function ψ

Has four distinguished values $\{\psi_s, \psi_g, \psi_i, \psi_l\} \subset \mathbf{R}^3$.
Takes on a continuum of values, but will still be non-smooth
Introduce the volume fraction of phase $\boldsymbol{p}$,

$$\boldsymbol{V}_p(\psi) = \begin{cases} \mathbf{1} & \psi = \psi_p, \\ \mathbf{0} & \psi = \psi_q, q \neq p \end{cases}$$

and is linear in ψ, so that $\boldsymbol{V}_s + \boldsymbol{V}_g + \boldsymbol{V}_i + \boldsymbol{V}_l = \mathbf{1}$ everywhere.

Local molar conc. of phase p is given by $c_p = \gamma_p V_p(\psi)$ and satisfies the conservation law

$$\partial_t c_p + \nabla \cdot (v c_p) = \sum_{k=1}^{N_r} R_k(U, \psi) s_k^p$$

N_r reactions with rates R_k and stoichiometric constant s_k^p for phase p.

Scalar transport

The phase function ψ fixes the local transport parameters. Solve

$$\partial_t U_j + \nabla \cdot (v U_j + [\mathcal{D}(U, \psi) \nabla U]_j) = \sum_{k=1}^{N_r} R_k(U, \psi) s_k^j$$

$\mathcal{D}$	Maxwell-Stefan, Poisson-Nerst, Ideal gas Law
R_k	Oxygen reduction, Carbon corrosion, Hydrogen oxidation, Liquid-vapor phase change
Interfacial transport	Henry's law, water uptake into ionomer, incorporated as interfacially supported reactions as opposed to BCs!

Validation

Cyclic Potential Sweeps
AC impedance
SAX experiments
Post-mortem carbon corrosion

Carbon Corrosion – Micron scale

Brian Wetton, G.S. Kim

Oxygen Reduction/Reverse Oxygen Reduction (o)	$O_2 + 4p^+ + 4e^- \rightleftharpoons 2H_2O$,
Hydrogen Oxidation/Hydrogen Evolution (h)	$H_2 \rightleftharpoons 2p^+ + 2e^-$,
Carbon Oxidation (c)	$C + 2H_2O \rightharpoonup 4p^+ + 4e^- + CO_2$

Common Electrode potential, for reaction r=o, h, c, at anode/cathode

$$
\begin{aligned}
\boldsymbol{E}_{a/c} &= \boldsymbol{E}_{r,ref} + \boldsymbol{N}_r(\boldsymbol{C}_o, \boldsymbol{C}_h) + \boldsymbol{\eta}_r(\boldsymbol{i}_r), \\
\boldsymbol{V}_{\text{cell}} &= \boldsymbol{E}_c - \boldsymbol{E}_a - \boldsymbol{R}_\Omega \boldsymbol{I}, \\
\boldsymbol{i}_r &= \boldsymbol{i}_{r,ref} \left\{ \exp\left(\frac{\boldsymbol{\alpha}_r \boldsymbol{\mathcal{F}} \boldsymbol{\eta}_r}{\boldsymbol{RT}} \right) - \exp\left(-\frac{(\boldsymbol{1} - \boldsymbol{\alpha}_r) \boldsymbol{\mathcal{F}} \boldsymbol{\eta}_r}{\boldsymbol{RT}} \right) \right\},
\end{aligned}
$$

$$
\begin{aligned}
\text{Small current} \quad & \boldsymbol{i}_r \approx \overbrace{\left(\boldsymbol{i}_{r,ref} \frac{\boldsymbol{\mathcal{F}}}{\boldsymbol{RT}} \right)}^{\boldsymbol{R}_r^{-1}} \boldsymbol{\eta}_r \\
\text{Large current} \quad & \boldsymbol{\eta}_r \approx \frac{\boldsymbol{RT}}{\boldsymbol{\alpha}_r \boldsymbol{\mathcal{F}}} \ln \frac{\boldsymbol{i}_r}{\boldsymbol{i}_{r,ref}}
\end{aligned}
$$

Each reaction competes to provide the local current $\boldsymbol{I}(\boldsymbol{x})$

$$\boldsymbol{I}(\boldsymbol{x}) = \boldsymbol{i}_c(\boldsymbol{x}) + \boldsymbol{i}_o(\boldsymbol{x}) + \boldsymbol{i}_h(\boldsymbol{x})$$

Oxidation reactions (producing electrons)	$\boldsymbol{i} > \boldsymbol{0}$ and $\boldsymbol{\eta} > \boldsymbol{0}$,
Reduction reactions (consuming electrons)	$\boldsymbol{i} < \boldsymbol{0}$ and $\boldsymbol{\eta} < \boldsymbol{0}$

Kinetic Parameters

Reaction	Nerst	E_{ref}	i_{ref}	α_r
Carbon Ox. (c)	-	0.207V	1.136×10^{-5} A/m^2	0.324
Hydrogen Ev. (h)	$C_{H_2}^{ref} = 100 \frac{\text{mol}}{\text{m}^3}$	0	$\eta_h = R_h i_h$	$R_h = 0.10\Omega$-cm^2
Oxygen Red. (o)	$C_{O_2}^{ref} = 40.9 \frac{\text{mol}}{\text{m}^3}$	1.28V	9.3×10^{-4} A/m^2	1.0
Rev. Ox. Red. $i_o > 0$	-		$\eta_o = R_o i_o$	$R_o = 0.01\Omega$-cm^2

Oxygen/Hydrogen cross over, $A = 3 \times 10^{-3}$ m/s,

$$J_r = A(C_{r,a} - C_{r,c})$$

Unknowns

Anode and Cathode catalyst layer conc.	$C_{o,a}, C_{h,a}$	$C_{o,c}, C_{h,c}$
Partial currents	$i_{o,a}, i_{h,a}, i_{c,a}$	$i_{o,c}, i_{h,c}, i_{c,c}$
Local current	$I(x)$	$I(x)$
Anode and Cathode potentials	E_{an}	E_{cat}

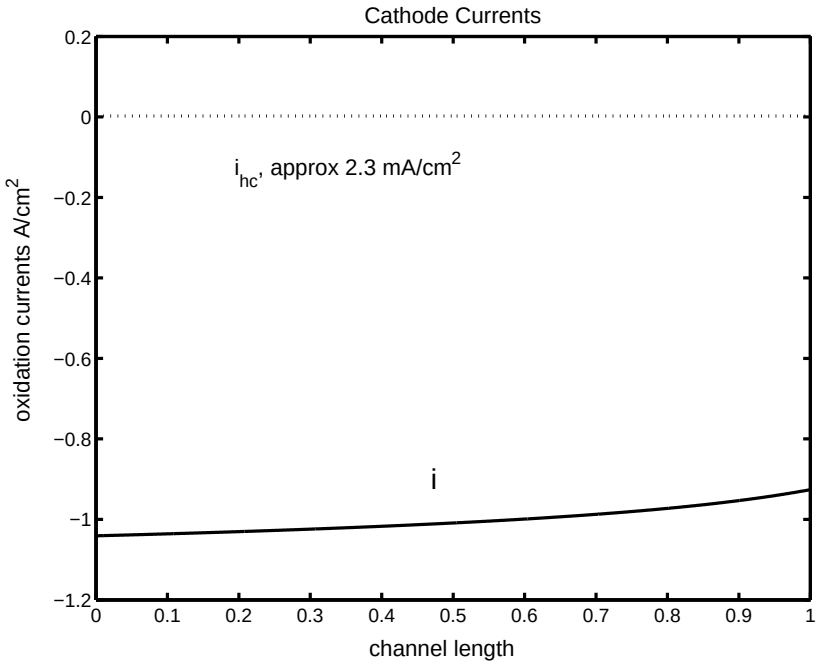

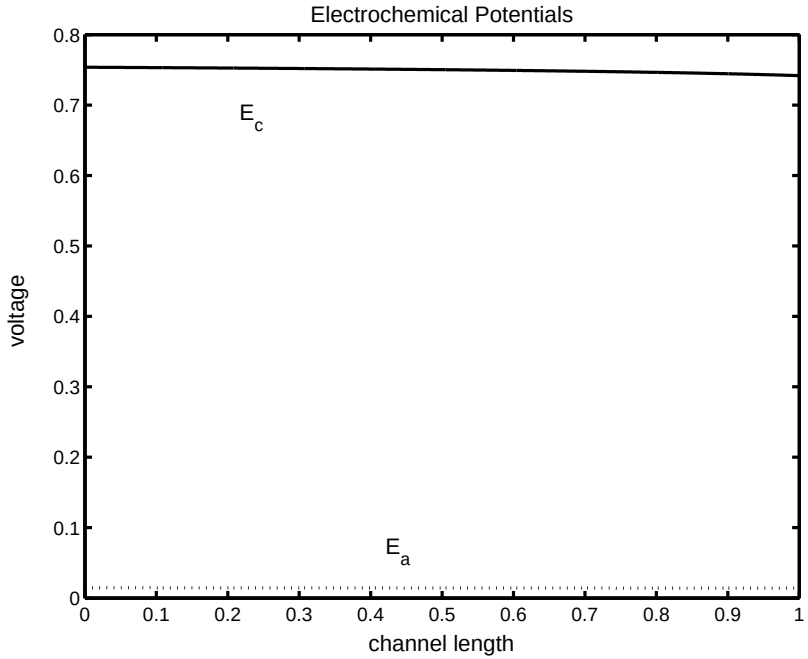

Base case– Coflow

An/Cat 2.2/2.0 barg, stoich=1.2/1.8, $\boldsymbol{I_T = 1}$ A/cm^2, $\boldsymbol{V_{\text{cell}} = 0.635V}$.

Small hydrogen oxidation current (2.3 mA/cm^2) on cathode due to hydrogen crossover. This current is present at open circuit and causes the drop in open circuit voltage from 1.28 to 0.95V.

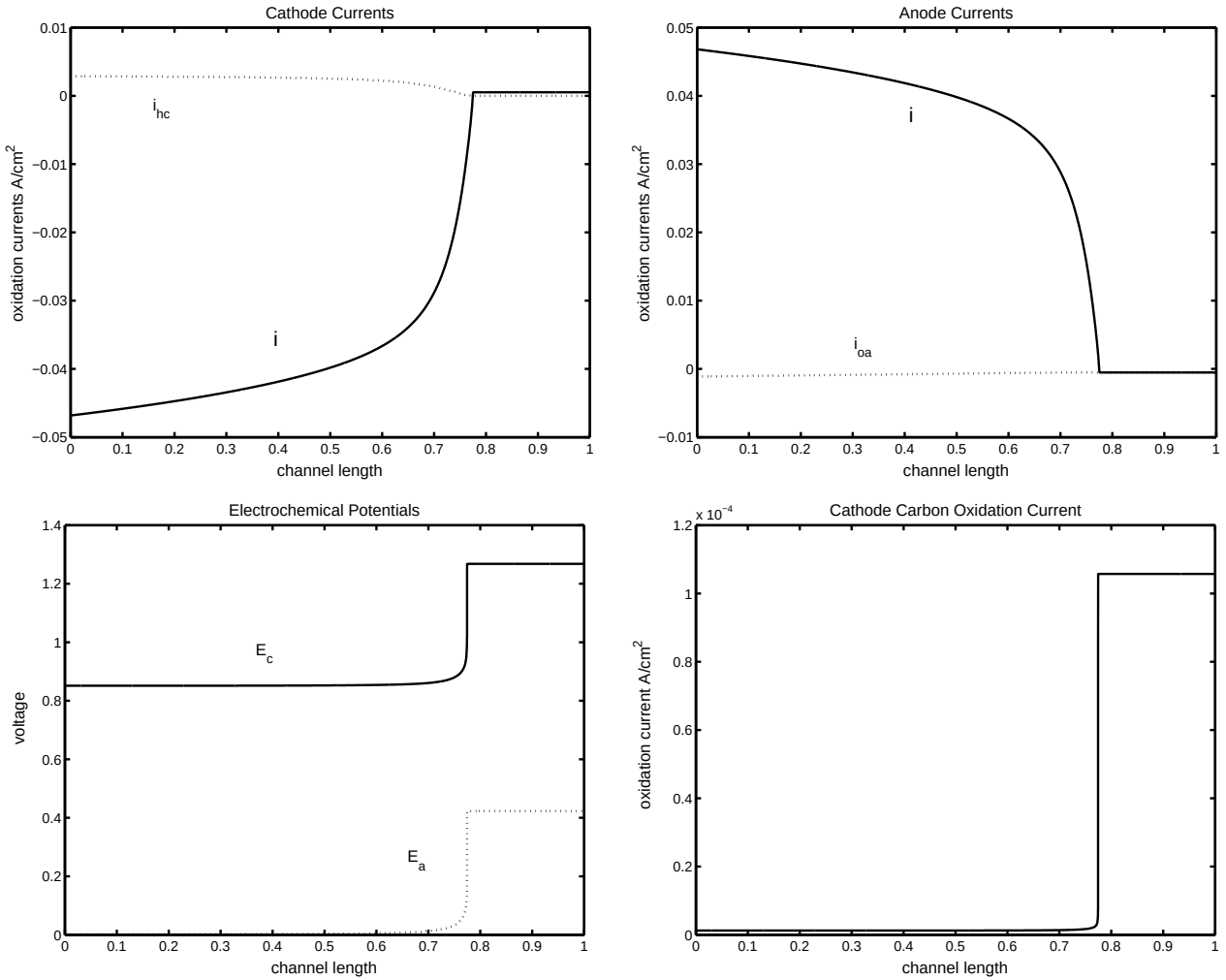

Partial Anode Understoich (idle)– Coflow (Reiser et. al.)

An/Cat 2.2/2.0 barg, stoich=1.1/1.8, $\boldsymbol{I_T = 30}$ mA/cm^2, $\boldsymbol{V_{\text{cell}} = 0.845V.}$

Hydrogen cross-over drives cell to anode understoich. Oxygen reduction at anode (from crossover) and Reverse Oxygen reduction at cathode. Elevated cathode pot leads to sig. carbon corrosion. (1 mg of carbon/hour = $\boldsymbol{6 \times 10^{-4}}$A).

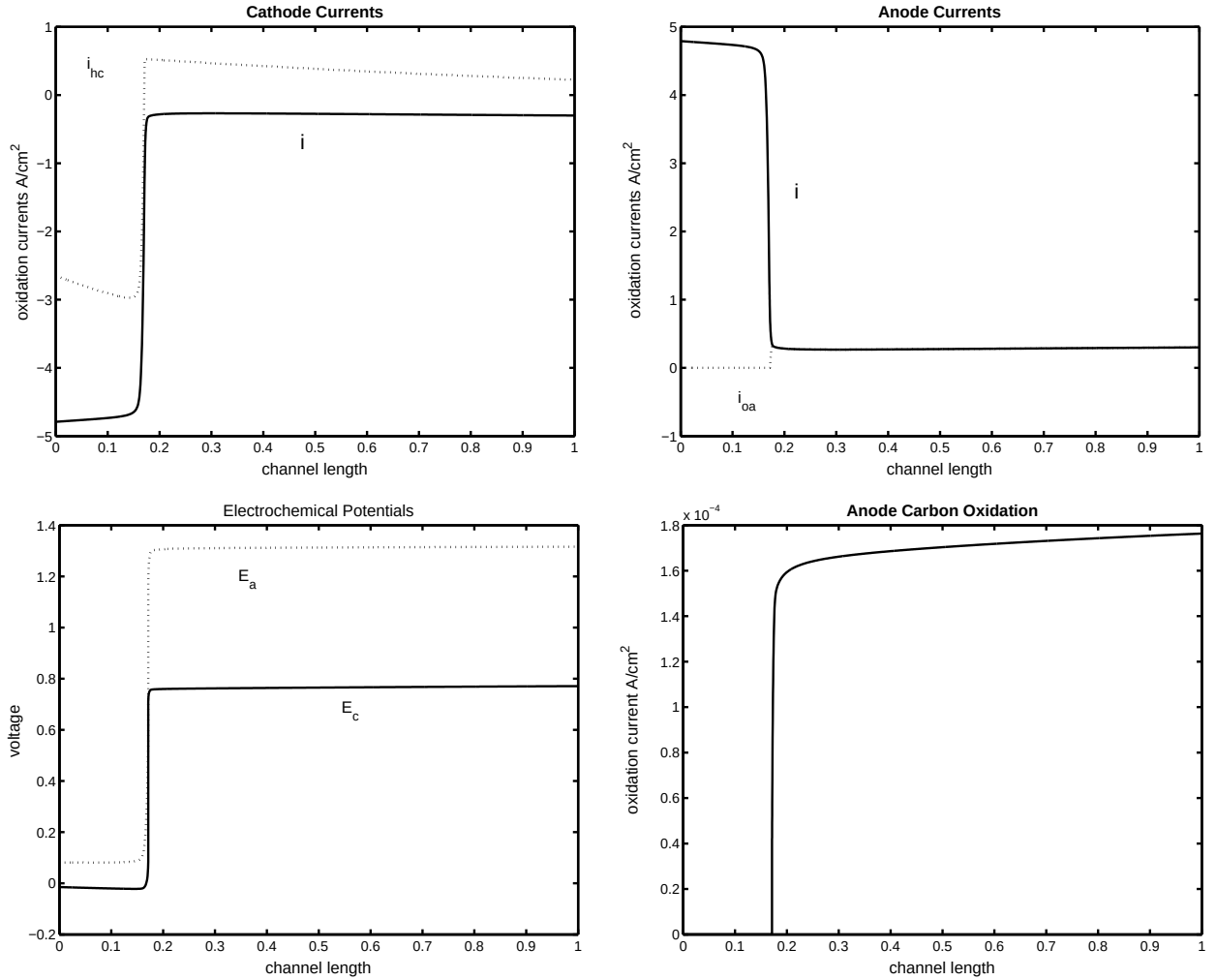

Anode Understoich – Coflow

An/Cat 2.2/2.0 barg, stoich=0.8/1.8, $\boldsymbol{I_T = 1}$ A/cm^2, $\boldsymbol{V_{\text{cell}} = -0.575V.}$

Current near inlet is limited only by hydrogen mass transfer on anode. On cathode oxygen reduction (at mass transfer limit) plus hydrogen evolution. After depletion of hydrogen, anode and cathode pot. rise, leading to reverse oxygen red. on anode, hydrogen oxidation and oxygen reduction on cathode.

Sp^3 Carbon Support Development

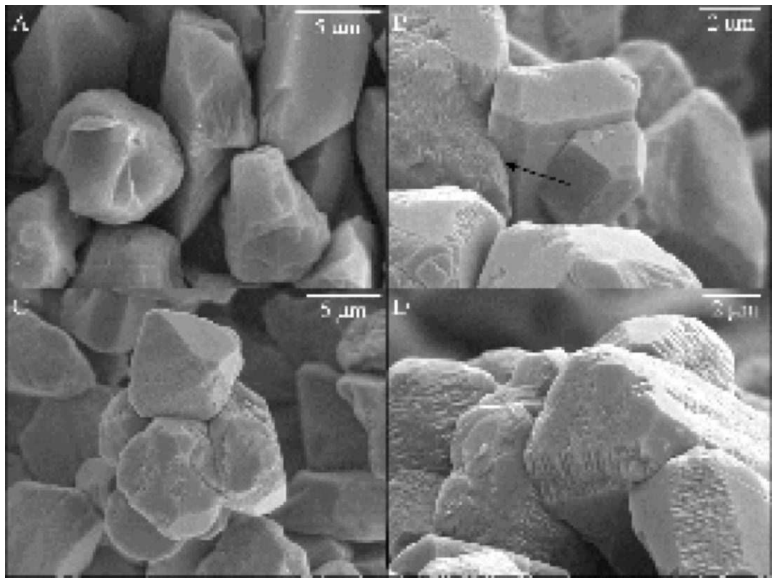

Replace reactive Sp^2 carbon (carbon black) with more inert Sp^3 (diamond)
Excellent dimensional stability and corrosion resistance
Inexpensive, $2/gram
Can be made electrically conductive with Boron doping
Bonds well to Pt

Conducting powder was prepared by coating insulating diamond powder (8-12 μm diam, 2 m^2/g) with a thin boron-doped overlayer using microwave plasma-assisted chemical vapor deposition. Deposition times from 1 to 6 h were evaluated. The surface area of this powder ($\approx$2 m^2/g) is lower than that desired for an ideal support (100 m^2/g)

(A) before diamond deposition, (B-D) after 1, 2, 6 hours of deposition.

Electrical resistance measurements of the bulk powder (no binder) confirmed that a conductive diamond overlayer formed, as the conductivity increased from near zero (insulating, $< 10^{-5}$ S/cm) for the uncoated powder to 1.5 S/cm after the 6-h growth.

Nanophase Models and Carbon Corrosion

Sp^2 support materials

- Where within the catalyst layer does carbon corrions occur?
- How much carbon corrosion is too much?
- How does liquid water impact carbon corrosion?

Sp^3 support materials

- How does the differing surface chemistry impact support/ionomer mixing and agglomeration?
- How much aggolomeration is needed to insure electronic conductivity?
- Will differing surface wetability change the interaction with liquid water?

Pt dissolution

Two principle mechanisms for Platinum loss in the catalyst layer have been proposed: surface migration and Pt dissolution/reprecipitation.
Patterson [2002] suggests that Pt dissolution is a major source of Pt surface area loss.
Yasuda [2006] has shown that potential cycling can induce Pt dissolution, that rates of dissolution are greatly impacted by molecular hydrogen concentrations, and the location of Pt deposits moves towards the anode with reduction of hydrogen concentration in the membrane

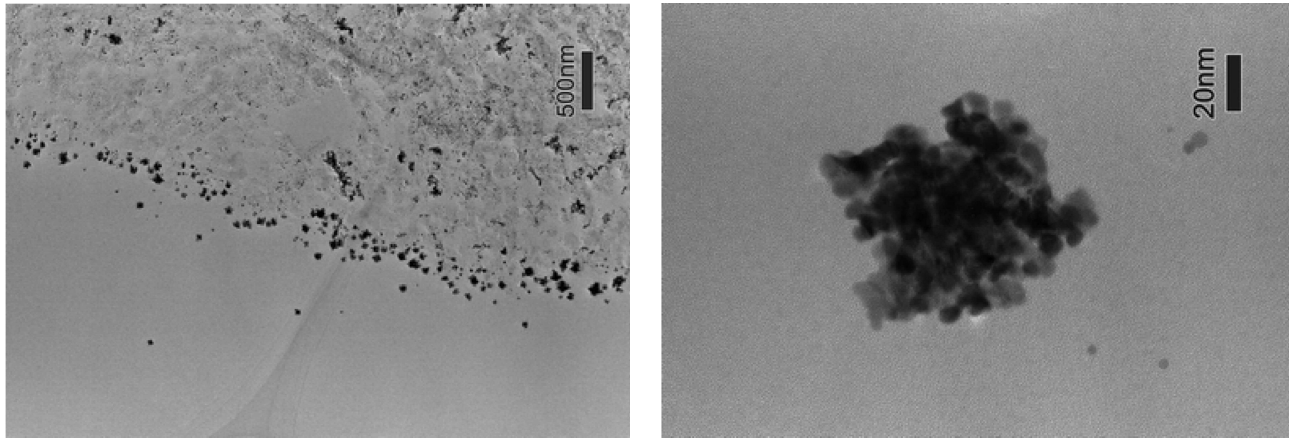

(Left) A TEM image of the interface between the cathode catalyst layer and the polymer electrolyte membrane of an MEA after a potential cycling test for 500 cycles under a nitrogen atmosphere (sample N-5). Potential cycling range: 0.1-1.2 V vs. SHE. (Right) Enlargement of deposited Pt particles. From Yasuda et al [2006].

Include extra phase for Pt metal, and extra reactions

$$\mathbf{Pt + H_2O \rightleftharpoons PtO + 2H^+ + 2e^-}$$

$$\mathbf{PtO + 2H^+ \rightleftharpoons Pt^{2+} + H_2O}$$